



OPEN ACCESS

EDITED BY

Ji-Feng Feng,
University of Chinese Academy of Sciences,
China

REVIEWED BY

Nguyen Quoc Khanh Le,
Taipei Medical University, Taiwan
Xue-Feng Leng,
University of Electronic Science and
Technology of China, China

*CORRESPONDENCE

Hongbing Duan
✉ dhb3100@sina.com
Sunkui Ke
✉ kesunflower@163.com

†These authors share first authorship

RECEIVED 03 March 2024

ACCEPTED 18 November 2024

PUBLISHED 17 February 2025

CITATION

Huang X, Jiang S, Li Z, Lin X, Chen Z, Hu C,
He J, Yan C, Duan H and Ke S (2025)
Prediction of right recurrent laryngeal
nerve lymph node metastasis in
esophageal cancer based on computed
tomography imaging histology.
Front. Oncol. 14:1388355.
doi: 10.3389/fonc.2024.1388355

COPYRIGHT

© 2025 Huang, Jiang, Li, Lin, Chen, Hu, He,
Yan, Duan and Ke. This is an open-access
article distributed under the terms of the
[Creative Commons Attribution License \(CC BY\)](https://creativecommons.org/licenses/by/4.0/).
The use, distribution or reproduction in other
forums is permitted, provided the original
author(s) and the copyright owner(s) are
credited and that the original publication in
this journal is cited, in accordance with
accepted academic practice. No use,
distribution or reproduction is permitted
which does not comply with these terms.

Prediction of right recurrent laryngeal nerve lymph node metastasis in esophageal cancer based on computed tomography imaging histology

Xiaoli Huang^{1,2†}, Shumin Jiang^{1†}, Zhe Li¹, Xiong Lin¹,
Zhipeng Chen¹, Chao Hu¹, Jianbing He¹, Chun Yan¹,
Hongbing Duan^{1*} and Sunkui Ke^{1*}

¹Department of Thoracic Surgery, Zhongshan Hospital of Xiamen University, Xiamen, Fujian, China,

²The School of Clinical Medicine, Fujian Medical University, Fuzhou, Fujian, China

Purpose: This study aimed to identify risk factors for right recurrent laryngeal nerve lymph node (RRLNLN) metastasis using computed tomography (CT) imaging histology and clinical data from patients with esophageal squamous cell carcinoma (ESCC), ultimately developing a clinical prediction model.

Methods: Data were collected from 370 patients who underwent surgical resection at the Department of Thoracic Surgery, Zhongshan Hospital of Xiamen University, from December 2014 to December 2020. Subsequently, the venous-stage chest-enhanced CT images of the patients were imported into 3DSlicer 4.11 software, allowing for the extraction of imaging histological features. Additionally, by combining the clinical data of the patients, single- and multifactor analyses were conducted to screen the risk factors and build a predictive model in the form of a nomogram. The area under the curve (AUC) was used as a discriminant for model accuracy, while differentiation and calibration methods were applied to further evaluate the model's accuracy. Finally, the Bootstrap resampling method was employed to repeat sampling 2,000 times to draw calibration curves, while the K-fold crossvalidation method was used for the internal validation of the prediction model.

Results: The RRLNLN lymph node metastasis rate was 17.3%. Four significant factors—Maximum2DDiameterSlice, Mean, Imc1, and Dependence Entropy—were identified. Alignment diagrams were subsequently constructed, yielding an AUC of 0.938 and a C-index of 0.904 during internal validation.

Conclusion: The model demonstrates high predictive accuracy, making it a valuable tool for guiding the development of preoperative protocols.

KEYWORDS

esophageal cancer, right recurrent laryngeal nerve lymph nodes, computed tomography imaging histology, nomogram, Area Under Curve (AUC), CT

1 Introduction

Esophageal cancer is the sixth leading cause of cancer-related deaths and the eighth most common cancer worldwide. It affects more than 450,000 people all over the world, and its incidence is rising rapidly each year. The general 5-year survival rate for esophageal cancer ranges from 15% to 25% (1). According to some data, approximately half of the global cases of esophageal cancer occur in China, which has the highest number of patients in the world. Moreover, esophageal cancer ranks third in incidence rate and fourth in mortality rate among all cancers, with an extremely low 5-year survival rate. Hence, there is an urgent need for better treatment options (2). The existing treatment modality for esophageal cancer is mainly based on surgical resection with lymph node dissection and adjuvant radiotherapy. Presently, adopting esophageal cancer resection with three-field lymphadenectomy can improve the 5-year survival rate to approximately 40%–55.6%. However, this surgical approach is associated with an increased risk of complications (3–7). In particular, the clearance of lymph nodes close to the right recurrent laryngeal nerve (8–10) is prone to result in complications such as aspiration pneumonia, as indicated by related data (11). Moreover, according to some studies, not all lymph node dissections can bring postoperative survival benefits (9, 10). Therefore, it is of great importance to perform a preoperative prediction on two key items: whether the lymph nodes adjacent to the right recurrent laryngeal nerve are metastatic and whether this information can guide the development of a surgical plan, determine the surgical access, and refine the intraoperative lymph node dissection strategy. Currently, the most effective and conventional method for predicting metastasis of right recurrent laryngeal nerve lymph (RRLNLN) in esophageal cancer is chest computed tomography (CT), with the short-axis diameter redefined from 10 mm to 6.5 mm by Bin Li (12). However, in this regard, no consensus has been reached in domestic and international literature regarding this criterion, and CT shows low accuracy and specificity in predicting positive lymph nodes. The concept of imaging histology was first introduced by Dutch scholar Lambin (13) in 2012. It involves the use of imaging technologies such as CT, positron emission tomography (PET), nuclear magnetic resonance imaging (MRI), and B-ultrasound. Through these technologies, high-throughput image data are extracted, enabling tumor segmentation, feature extraction, and model building. This approach assists physicians in making the most accurate diagnosis by giving deeper mining, prediction, and analysis of the massive image data information. Considering the heterogeneity of tumors, imaging histology can be used in exploring the imaging data of patients, aiming at finding the internal characteristics of tumors and further reflecting the changes in the human microenvironment, cytological morphology, and gene level, thus affecting the diagnosis, treatment, and prognosis of diseases finally (14). At present, imaging features are extensively utilized in various fields of medical research, including the extended prediction of cerebral hemorrhage (15) and the development and verification of CT-based imaging features for predicting the overall survival of multiorgan tumors (16). This work aimed to predict the metastasis of RRLNLN

and provide guidance for surgical planning by combining clinical data and imaging histological features of the patients.

2 Materials and methods

2.1 Materials

A total of 789 patients who underwent radical surgery for thoracic segmental esophageal cancer at the Department of Thoracic Surgery, Zhongshan Hospital of Xiamen University, from December 2014 to December 2020, were included in this retrospective analysis. After excluding those who did not meet the inclusion criteria, 367 patients were finally included in this study.

2.1.1 Inclusion criteria

The inclusion criteria were as follows: (1) Patients were diagnosed with esophageal squamous carcinoma before surgery, and their data were complete and nondeficient, kept in the relevant electronic files or archived. (2) Patients accepted the relevant preoperative examinations, such as chest-enhanced CT, abdomen-enhanced CT, ECT, and neck ultrasound, to exclude distant metastases. (3) Patients underwent radical esophageal cancer surgery, including two- or three-field clearance, and pathological results indicated complete resection of the RRLNLN. (4) Patients received a chest CT enhancement scan at our hospital 3 weeks before surgery, and the image quality was clear enough to be exported in DICOM format.

2.1.2 Exclusion criteria

The exclusion criteria were as follows: (1) Clinical examination data of the patients were missing, or the patients were examined outside the hospital. (2) Patients received preoperative neoadjuvant therapies, such as radiotherapy, chemotherapy, and immune-targeted therapy (pathological results of the patients changed after surgery, thus causing errors in the experimental results). (3) Patients suffered other malignant tumors in combination. (4) The RRLNLN was not identified in the patients, as confirmed by two pathologists and thoracic surgeons through analysis of the specimens obtained intraoperatively. (5) The esophageal cancer was located outside the thoracic segment, and the pathology was of a type other than squamous carcinoma.

2.2 Quantitative analysis of lymph node images

As shown in [Figure 1](#), the high-quality and standardized CT images were first obtained in Digital Imaging and Communications in Medicine (DICOM) file format. Successively, these DICOM files were imported into 3DSlicer 4.11 software for automatic segmentation of the region of interest (ROI). Afterward, the lymph nodes were segmented into ROI regions by using a threshold segmentation method, followed by manual outlining of the ROI regions by two experienced thoracic surgeons. Finally, the

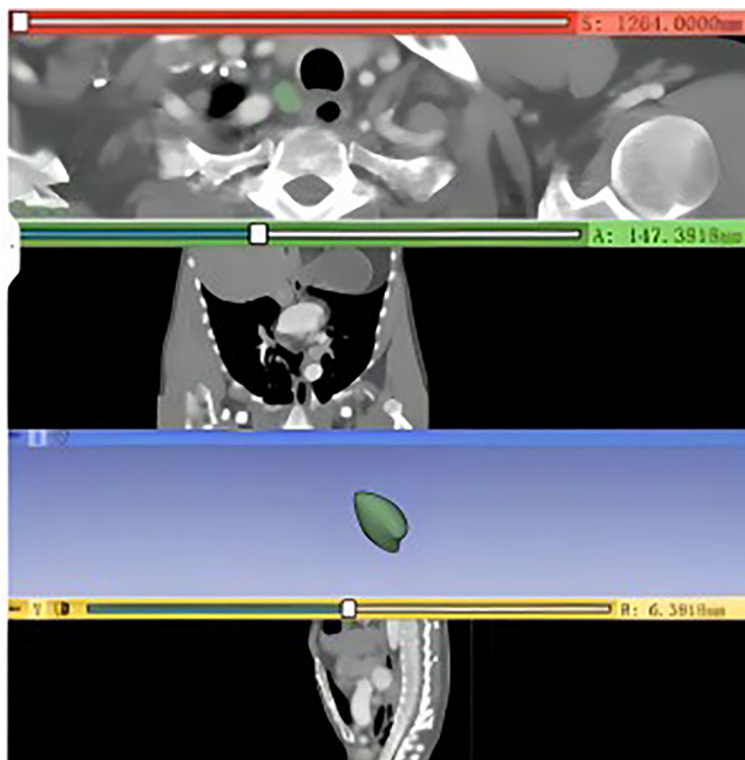


FIGURE 1
CT 3D reconstruction of the RRLN.

outlined lymph nodes were given three-dimensional (3D) reconstruction, and high-throughput imaging features of the lymph nodes were automatically extracted and calculated using Radiomics. These features included first-order histogram features, morphological features, and parameters related to second- and high-order textural features, as well as the relationship between the lymph nodes and surrounding tissues. Based on the Radiomics analysis, a total of 130 imaging features were ultimately obtained.

2.3 Statistical analysis

Statistical analysis was conducted using R3.6.1 software. The count data were expressed as percentages, and the Chi-square test was performed for comparisons between groups. Normally distributed measures were presented as mean \pm standard deviation, and two independent samples *t*-tests were used for comparisons between groups. The measures with skewed distribution were described by median and interquartile spacing, with the Mann–Whitney *U* test (Wilcoxon rank-sum test) used for comparisons between groups. Univariate analysis was performed on the demographic and clinical characteristics of the patients, and variables with $p < 0.05$ were included in the Lasso-logistic regression for variable screening, along with the imaging histological features extracted using Radiomics. Therefore, Lasso-logistic regression was performed by plotting the receiver operating characteristic curve (ROC) and calculating the area under the curve (AUC) to evaluate the model's discrimination. The AUC value ranges from 0.5 to 1, with a value

closer to 1 indicating better model discrimination and higher prediction accuracy. The predictors corresponding to the maximum AUC were chosen, and variables were screened using logistic regression and Lasso-logistic regression models, with predictors further filtered using the stepwise method. Additionally, internal validation of the model was performed using 10-fold crossvalidation. The R3.6.1 software rms package was used in building the alignment diagram prediction model. The Bootstrap method was used to repeat the sampling 2,000 times, generating the calibration curve for the internal validation of the alignment diagram model. Additionally, Harrell's C-statistic was adopted to calculate the consistency index (C-index), assessing the discrimination of the alignment diagram model. All analyses were tested bilaterally, and statistical differences exhibited a two-sided $p < 0.05$.

3 Results

3.1 General characteristics of the cases

In this retrospective analysis, clinical study data from a total of 367 patients were obtained, as displayed in Table 1. Based on the metastasis of RRLN, patients were divided into two groups: metastatic ($n = 67$) and nonmetastatic ($n = 300$). As indicated by univariate analysis, five factors showed statistical significance ($p < 0.05$) between the two groups: the pathological type of hypofractionation, the longest diameter of lymph nodes, the lymph node plain CT value, the tumor plain CT value, and the tumor enhancement CT value. However, no

TABLE 1 Differences in demographic and clinical characteristics between the two groups.

Variables	Total	Metastatic group	Nonmetastatic group	t/χ^2	p -value
Gender					
Man	300 (81.74)	250 (82.51)	50 (78.13)	0.68	0.409
Woman	67 (18.26)	53 (17.49)	14 (21.88)		
Age (years)	61.28 ± 8.24	61.6 ± 7.97	59.73 ± 9.31	1.653	0.099
Smoking history					
Yes	258 (69.73)	217 (70.92)	41 (64.06)	1.178	0.278
None	112 (30.27)	89 (29.08)	23 (35.94)		
Tumor	3.8 ± 1.54	3.75 ± 1.59	4 ± 1.27	- 1.383	0.169
Longest diameter (cm)					
Tumor location	18 (4.86)	13 (4.25)	5 (7.81)	3.811	0.149
Upper	251 (67.84)	204 (66.67)	47 (73.44)		
Middle	101(27.30)	89(29.08)	12(18.75)		
Lower					
Degree of differentiation	9 (2.43)	8 (2.61)	1 (1.56)	-	0.001
Low	334 (90.27)	283 (92.48)	51 (79.69)		
Medium	27 (7.30)	15 (4.90)	12 (18.75)		
High	0.56 (0.5, 1)	0.55 (0.4, 0.7)	1.3 (1.1, 1.85)	11.027	< 0.001
Lymph node	35.35 ± 22.81	33.97 ± 23.09	42.06 ± 20.26	- 2.582	0.01
Longest diameter (cm)	62.84 ± 15.59	62.79 ± 15.43	63.1 ± 16.45	- 0.147	0.883
Lymph node plain CT value	19.9 ± 20.05	18.23 ± 20.74	27.85 ± 13.99	- 4.552	< 0.001
Lymph node enhancement CT value	39.12 ± 10.73	39.85 ± 10.77	35.66 ± 9.92	2.862	0.004

$p < 0.05$ indicates that the difference is statistically significant.

statistically significant correlation was found between lymph node metastasis and other factors.

3.2 Lasso-logistic regression screening variables

As shown in Figures 2, 3, variables with $p < 0.05$ from univariate analysis were included in Lasso-logistic regression for variable screening, alongside 130 imaging histological features. The Lasso-logistic regression analysis identified five variables with the maximum AUC value of 0.938: Mean, Maximum2DDiameterSlice, Imc1, Run Length Nonuniformity, and Dependence Entropy.

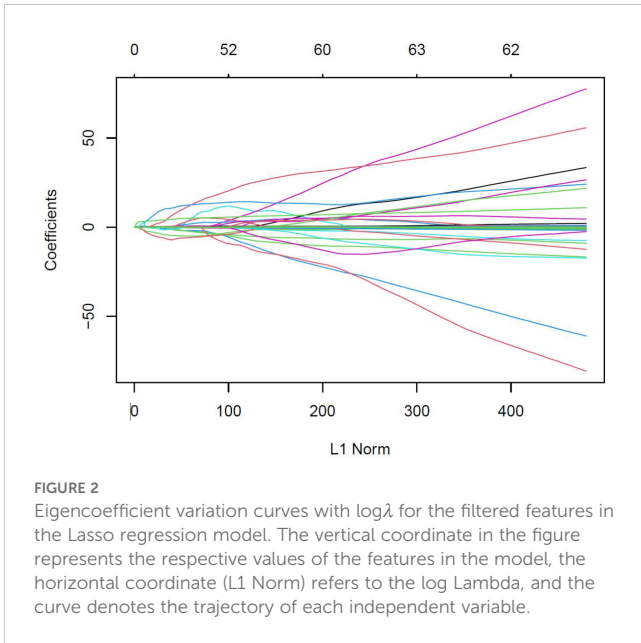
3.3 Results of logistic regression model analysis

The five variables (Mean, Maximum2DDiameterSlice, Imc1, Run Length Nonuniformity, and Dependence Entropy), which were

screened using Lasso-logistic regression and the stepwise method, were included in the multifactor logistic regression analysis, with the results presented in Table 2. Based on the results from the multifactor logistic regression analysis, the prediction model was established with the following equation.

$$p(\text{MPositive}) = \frac{e^{\left(\frac{-15.861-0.004 \times \text{Mean} + 0.520 \times \text{Maximum2DDiameterSlice}}{+0.079 \times \text{Imc1} + 1.154 \times \text{DependenceEntropy}}\right)}}{1 + e^{\left(\frac{-15.861-0.004 \times \text{Mean} + 0.520 \times \text{Maximum2DDiameterSlice}}{+0.079 \times \text{Imc1} + 1.154 \times \text{DependenceEntropy}}\right)}}$$

In our study, four imaging features (Mean, Maximum2DDiameterSlice, Imc1, Run Length Nonuniformity, and Dependence Entropy) were selected through the multivariate logistic regression model. These four predictors were then used to construct a nomogram model for predicting right recurrent laryngeal lymph node metastasis in esophageal cancer, enabling the prediction model to be transformed into a practical application tool. For example (Figure 3), the column diagram shows that the point (score) in the first row represents the score reference for each variable, and the total points represent the total score added by the scores corresponding to the values of all predictors. The predicted value



represents the positive prediction probability, and the total score can be mapped to the linear predicted value based on the total points, thereby obtaining the probability of the patient's right recurrent laryngeal lymph node metastasis. As shown in the figure below, a patient is considered positive when the total score is ≥ 220 ($p(\text{positive}) \geq 0.40$).

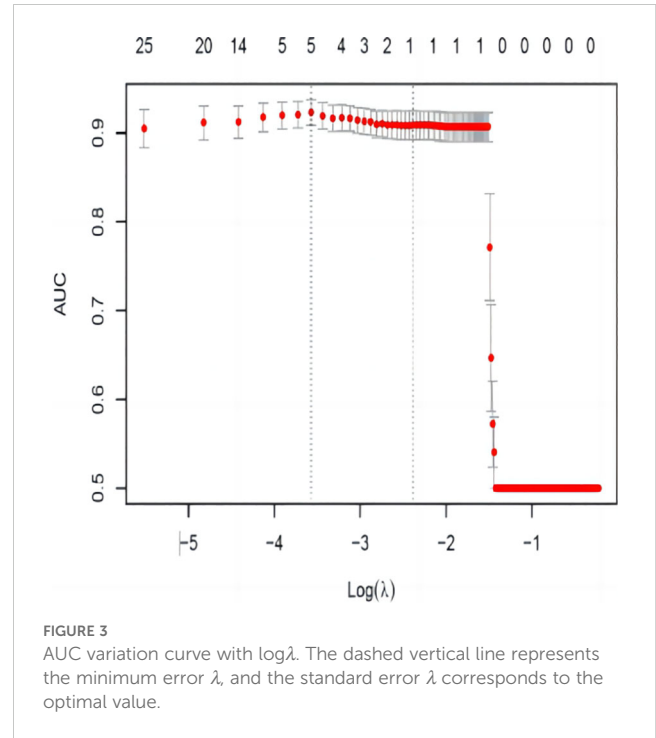
3.4 Validation of model accuracy for predicting RRLNLN metastasis in esophageal cancer

In this work, the ROC curve of the model was plotted, with an AUC value of 0.938 (95% CI = 0.909 to 0.967, $p < 0.001$), as shown in Figure 4. Therefore, the AUC value of 0.938, being greater than 0.9, indicates that the present prediction model has high accuracy and is considered positive when $p(\text{positive}) \geq 0.15$ (i.e., the critical value). The Brier score of the model, calculated using R language, was 0.071, which is less than 0.25. The prediction results accorded well with the actual outcomes, indicating a high calibration degree of the model.

3.5 Internal validation of the model for predicting RRLNLN metastasis in esophageal cancer

In this work, the Bootstrap resampling method and K-fold crossvalidation were used for the internal validation of the prediction model.

As indicated in Figure 5, the dashed line represents the prediction result of the model, with the horizontal coordinate referring to the predicted positive probability and the vertical



coordinate denoting the actual positive probability. Moreover, the dashed line (apparent) represents the result of internal validation, the 45° curve (ideal) refers to the perfect prediction of an ideal model, and the solid line (bias-corrected) indicates the bias-corrected result. As observed, the solid line and the dashed line overlapped almost completely, suggesting good internal validation of the model. The C-index of the prediction model was 0.904, with a mean absolute error of 0.008, indicating the high accuracy of the model in predicting RRLNLN metastasis in esophageal cancer.

In this work, the accuracy of the prediction model was evaluated using 10-fold crossvalidation, with the results presented in Table 3. According to the table, the accuracy of the model in the training set was 83.16%, the sensitivity was 91.65%, the specificity was 81.37%, the positive predictive value was 50.84%, and the negative predictive value was 97.90%. Moreover, the accuracy in the validation set was 81.64%, with a sensitivity of 91.55%. Additionally, the specificity was 80.67%, the positive predictive value was 50.71%, and the negative predictive value was 97.19%. As indicated, the results of the training and validation sets were similar, suggesting the high accuracy of the prediction model.

3.6 Establishment and use of a nomogram for predicting RRLNLN metastasis in esophageal cancer

As exhibited in the nomogram of Figure 6, the point in the first row represents the score reference for each variable, the total points refer to the total score derived from all the predictive factors, and the predicted value denotes the probability of a positive prediction.

TABLE 2 Multivariate analysis of imaging parameters for predicting RRLNLN metastasis.

Variables	β	Standard error	Wald χ^2	p-value	OR (95% CI)
Constant	- 15.861	2.731	33.719	< 0.001	
Mean	- 0.004	0.001	13.542	< 0.001	0.996 (0.994,0.998)
Maximum 2D diameter slice	0.52	0.103	25.229	< 0.001	1.682 (1.373,2.060)
Imc1	0.079	0.034	5.338	0.021	1.083 (1.012,1.158)
Dependence entropy	1.554	0.429	13.145	< 0.001	4.733 (2.042,10.966)

p < 0.05 indicates that the difference is statistically significant.

Therefore, the total score can be mapped to the linear score via the total points, thereby determining the probability of RRLNLN metastasis in the patient. According to the figure below, a patient was considered positive when the total score was not less than 202 (p(positive) ≥ 0.15).

4 Discussion

Esophageal lymphatic vessels form a lymphatic network in the lamina propria and submucosa, spreading across the intermuscular space (17, 18). The submucosal lymphatic network is present in the right tracheoesophageal groove and has a direct connection with the RRLNLN, as indicated (17, 19). Lymph nodes near the RRLN are more prone to metastasis compared with other groups of lymph nodes. Considering the special structure of the right recurrent laryngeal nerve, complications such as hoarseness, respiratory issues, anastomotic fistula, and atrial fibrillation can arise during its clearance. Therefore, preoperative determination of RRLNLN metastasis is crucial in the survival and prognosis of the patients.

Given the deep location of the RRLNLN, imaging modalities such as CT, MR, ultrasound, PET-CT, and EUS are the most conventional methods for preoperative metastasis determination. However, numerous studies indicate that PET-CT/CT provides a low reference value for RRLNLN metastasis (20–22). In recent years, with the increasing application of prediction models in clinical practice, many experts and scholars have developed models for predicting lymph node metastasis based on CT imaging features. Jing (23) draw a metastasis prediction model by combining imaging features, identifying four types of imaging parameters associated with lymph node metastasis: shape features, size features, intensity histogram, and textural features. Larger lymph node volumes are more likely to be invaded by tumors, as demonstrated in previous studies (24, 25). Among the textural features, one primarily indicates the complexity the tumor’s internal structure, which is closely associated with tumor activity and prognosis (26). Using this method, a clinical prediction model is innovatively constructed by extracting imaging features to predict lymph node metastasis. However, the AUC value of this model is only 0.79, suggesting low accuracy. Moreover, the model includes 11 predictors despite having only a few cases, making it challenging to apply clinically.

In this work, a new imaging histology model was developed using high-resolution enhanced CT images from our patients. Moreover, 3D Slicer 4.11 software was used to outline the RRLNLN in the original

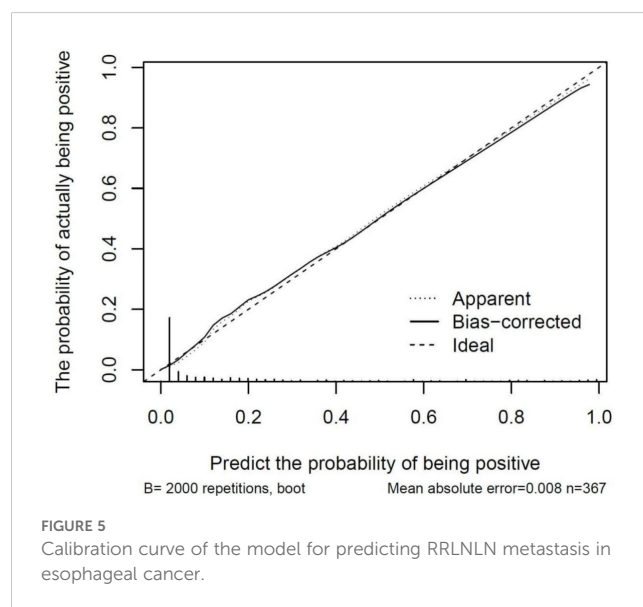
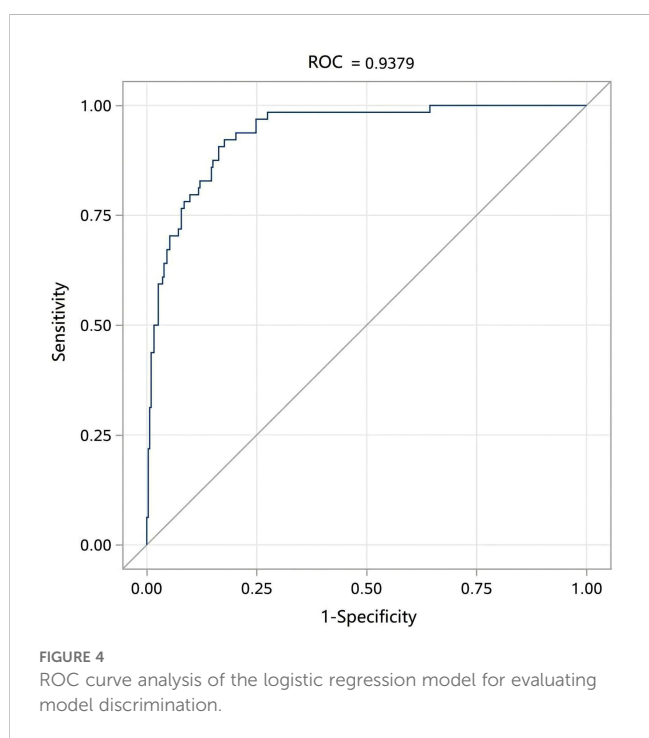


TABLE 3 Tenfold crossvalidation of the model for predicting RRLNLN metastasis.

	Accuracy (%)	Sensitivity (%)	Specificity (%)	Positive predictive value (%)	Negative predictive value (%)
Training set	83.16	91.65	81.37	50.84	97.90
Validation set	81.64	91.55	80.67	50.71	97.19

$p < 0.05$ indicates that the difference is statistically significant.

DICOM format of the CT images, realizing 3D reconstruction. Applying the Radiomics plug-in, the software automatically calculated the lymph node morphology, the textural features, and other relevant parameters, thereby facilitating the prediction of metastasis probability in the RLNLN. To address variable selection, the model complexity was adjusted to avoid overfitting and underfitting. Hence, Lasso-logistic regression was employed for multifactor analysis based on single-factor analysis, followed by a stepwise screening method to identify predictors corresponding to the maximum AUC. This approach maximized the scientific validity and accuracy of the screening process, ultimately leading to the construction of the alignment diagram for the prediction model. Simultaneously, the accuracy and consistency of the model were evaluated in the experiment. The results of the internal validation indicated that the alignment diagram could be widely used for preoperatively predicting RRLNLN metastasis of the right recurrent laryngeal nerve. Compared to previous methods, this approach was more intuitive and accurate. An AUC higher than 0.90 is generally considered highly accurate, and the AUC of this prediction model reached 0.938, indicating high accuracy. Moreover, according to relevant data, an internal validation C-index of 0.9 is also deemed highly accurate, and this model achieved a C-index of 0.904.

In this work, statistical analysis was conducted on a series of clinical data included in our univariate analysis, identifying five statistically significant factors (pathological type of hypofractionation): the longest diameter of lymph nodes, the lymph node plain CT value, the tumor plain CT value, the tumor enhancement CT value, and the longest diameter of lymph nodes. These findings are consistent with the results obtained in a previous study (27). Moreover, according to the statistical analysis, a strong correlation was found between the probability of lymph node metastasis and the pathological type of tumor, especially when the tumor was hypodifferentiated, as reported in previous studies (28, 29). The degree of tumor differentiation is more likely an independent risk element for thoracic lymph node metastasis in esophageal cancer, as it is negatively correlated with the rate of

lymph node metastasis. A lower degree of differentiation indicates a higher degree of malignancy and a higher rate of lymph node metastasis. In this work, the CT values of tumor and lymph nodes were innovatively incorporated, including scan and enhancement CT values. Moreover, to explore the accuracy of the results, three target areas with the same scan and enhancement images were selected. The CT values of these areas were measured and averaged to obtain the final results. The CT value reflects the density of the object, and changes in density can be used to analyze the composition of the tumor. Generally, tumors are primarily composed of soft tissue, with CT values ranging from 30 to 100. Thus, the CT values of the tumor and lymph nodes were considered factors in this work. Statistical analysis indicated a close relationship between the CT values and RRLNLN metastasis.

In contrast to evaluation based solely on manual reading, the analysis of RRLNLN using imaging histological features was more comprehensive and refined. Moreover, by reconstructing the structure of the lymph nodes, the morphological and textural features were more adequately captured. Finally, a total of four imaging features were derived: the maximum two-dimensional (2D) diameter (slice) in the shape feature, the mean value in the first-order feature, the grayscale dependence entropy in the correlation matrix (GLCM) feature, and the correlation information measure 1 in the grayscale covariance matrix feature. These were identified as predictors for RRLNLN metastasis. In Radiomics, each of the four features represents the internal structure of the tumor. A larger value of the maximum 2D diameter (slice) in the shape feature represents more information contained in the image space. Therefore, uniform pixels arranged around a lymph node with a larger diameter may be associated with tumor metastasis components. First-order features, also known as voxel intensity features, are related to the gray-level frequency distribution within the painted target area. The mean value is usually used to describe the distribution of voxels in the target area, revealing the solid component of the lymph nodes. The GLCM is commonly employed to describe the two-by-two arrangement of

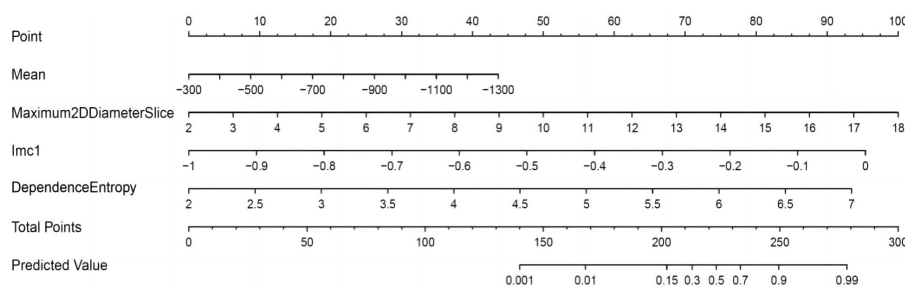


FIGURE 6 Nomogram for predicting RRLNLN metastasis in esophageal cancer.

voxels, with dependence entropy serving as a measure of the dependency on pro-domain intensity values. It also assesses the uniformity of image texture and the degree of randomness. It has been indicated that highly aggressive tumors with inhomogeneous internal echogenicity and enhanced entropy features in the texture show a stronger correlation with molecular typing (30). As a common method for describing texture by exploring the spatial correlation properties of the grayscale, the grayscale covariance matrix can reveal the content of real components contained within the tumor, specifically the number of tumor components present.

There are still limitations in this work. First, it is based on a single-center retrospective study with a relatively small sample size. Therefore, further prospective studies and multicenter studies with larger sample sizes are needed for training and validation. Second, the RRLNLN is small on the enhanced CT images, and some surrounding fat could not be eliminated even after correction by experienced technologists and clinicians. Therefore, further development of medical imaging technology and improvements in the accuracy and precision of tumor segmentation are required. Moreover, due to the lack of a larger public database, this model has only been internally validated, and further external validation is still pending.

5 Conclusion

3D Slicer 4.11 software was used to outline the ROI of lymph nodes, and imaging features were extracted from the ROI, including shape features, texture pattern heterogeneity, and intensity distribution. Moreover, a statistical method was employed to identify predictors for RRLNLN metastasis, and an alignment graph model was successfully constructed to predict RRLNLN metastasis preoperatively, thereby guiding the surgeon's surgical plan and the patient's prognosis for survival.

Data availability statement

The raw data supporting the conclusions of this article will be made available by the authors, without undue reservation.

Ethics statement

The studies involving humans were approved by Zhongshan Hospital Affiliated to Xiamen University. The studies were conducted in accordance with the local legislation and institutional requirements. Written informed consent for participation was not required from the participants or the participants' legal guardians/next of kin in accordance with the national legislation and institutional requirements.

Author contributions

XH: Conceptualization, Data curation, Formal analysis, Funding acquisition, Investigation, Methodology, Project administration,

Resources, Software, Supervision, Validation, Visualization, Writing – original draft, Writing – review & editing. SJ: Conceptualization, Data curation, Formal analysis, Investigation, Methodology, Project administration, Software, Supervision, Validation, Writing – original draft, Writing – review & editing. ZL: Conceptualization, Data curation, Formal analysis, Investigation, Methodology, Project administration, Software, Supervision, Validation, Writing – original draft, Writing – review & editing. XL: Conceptualization, Data curation, Formal analysis, Investigation, Methodology, Project administration, Software, Supervision, Validation, Writing – original draft, Writing – review & editing. ZC: Conceptualization, Data curation, Formal analysis, Investigation, Methodology, Project administration, Software, Supervision, Validation, Writing – original draft, Writing – review & editing. CH: Conceptualization, Data curation, Formal analysis, Investigation, Methodology, Project administration, Software, Supervision, Validation, Writing – original draft, Writing – review & editing. JH: Conceptualization, Data curation, Formal analysis, Investigation, Methodology, Project administration, Software, Supervision, Validation, Writing – original draft, Writing – review & editing. CY: Conceptualization, Data curation, Formal analysis, Investigation, Methodology, Project administration, Software, Supervision, Validation, Writing – original draft, Writing – review & editing. HD: Conceptualization, Data curation, Formal analysis, Funding acquisition, Investigation, Methodology, Project administration, Resources, Software, Supervision, Validation, Visualization, Writing – original draft, Writing – review & editing. SK: Conceptualization, Data curation, Formal analysis, Funding acquisition, Investigation, Methodology, Project administration, Resources, Software, Supervision, Validation, Visualization, Writing – original draft, Writing – review & editing.

Funding

The author(s) declare financial support was received for the research, authorship, and/or publication of this article. This work was supported by the Fujian Provincial Natural Science Foundation Projects (2018J01397) and the projects of the Xiamen Science and Technology Commission (502Z20184032).

Acknowledgments

We are grateful to Mr. Zhipeng Chen at Zhongshan Hospital of Xiamen University for his active work in the preparation of histological sections. We also thank Dr. Sunkui Ke and Dr. Hongbin Duan at Zhongshan Hospital of Xiamen University for their assistance in the preparation of the figures.

Conflict of interest

The authors declare that the research was conducted in the absence of any commercial or financial relationships that could be construed as a potential conflict of interest.

Publisher's note

All claims expressed in this article are solely those of the authors and do not necessarily represent those of their affiliated

organizations, or those of the publisher, the editors and the reviewers. Any product that may be evaluated in this article, or claim that may be made by its manufacturer, is not guaranteed or endorsed by the publisher.

References

- Sung H, Ferlay J, Siegel RL, Laversanne M, Soerjomataram I, Jemal A, et al. Global cancer statistics 2020: GLOBOCAN estimates of incidence and mortality worldwide for 36 cancers in 185 countries. *CA Cancer J Clin.* (2021) 71(3):209–49. doi: 10.3322/caac.21660
- Liu CQ, Ma YL, Qin Q, Wang PHK, Luo Y, Xu PF, et al. Epidemiology of esophageal cancer in 2020 and projections to 2030 and 2040. *Thorac Cancer.* (2023) 14(1):3–11. doi: 10.1111/1759-7714.14745
- Wang Y, Jiang Z, Xu C, Wang H, Tan L, Su J, et al. Increased MET gene copy number negatively affects the survival of esophageal squamous cell carcinoma patients. *BMC Cancer.* (2019) 19(1):240. doi: 10.1186/s12885-019-5450-6
- Tang J, Zhao JZ, Ren KM, Zheng FS, Wang XW, Liu HJ, et al. Risk factors of atrial fibrillation occurring after radical surgery of esophageal carcinoma. *J Cardiothorac Surg.* (2019) 14(1):60. doi: 10.1186/s13019-019-0885-z
- Chao YK, Chiu CH, Liu YH. Safety and oncological efficacy of bilateral recurrent laryngeal nerve lymph-node dissection after neoadjuvant chemoradiotherapy in esophageal squamous cell carcinoma: a propensity-matched analysis. *Esophagus.* (2020) 17:33–40. doi: 10.1007/s10388-019-00688-7
- Ye T, Sun Y, Zhang Y, Zhang Y, Chen H. Three-field or two-field resection for thoracic esophageal cancer: a meta-analysis. *Ann Thorac Surg.* (2013) 96:1933–41. doi: 10.1016/j.athoracsur.2013.06.050
- Shang QX, Chen LQ, Hu WP, Deng HY, Yuan Y, Cai J. Three-field lymph node dissection in treating the esophageal cancer. *J Thorac Dis.* (2016) 8:E1136–49. doi: 10.21037/jtd.2016.10.20
- Taniyama Y, Miyata G, Kamei T, Nakano T, Abe S, Katsura K, et al. Complications following recurrent laryngeal nerve lymph node dissection in oesophageal cancer surgery. *Interact Cardiovasc Thorac Surg.* (2015) 20(1):41–6. doi: 10.1093/icvts/ivv336
- Koterazawa Y, Oshikiri T, Takiguchi G, Hasegawa H, Yamamoto M, Kanaji S, et al. Prophylactic cervical lymph node dissection in thoracoscopic esophagectomy for esophageal cancer increases postoperative complications and does not improve survival. *Ann Surg Oncol.* (2019) 26(9):2899–904. doi: 10.1245/s10434-019-07499-1
- Ma GW, Situ DR, Ma QL, Long H, Zhang LJ, Lin P, et al. Three-field vs two-field lymph node dissection for esophageal cancer: a meta-analysis. *World J Gastroenterol.* (2014) 20(47):18022–30. doi: 10.3748/wjg.v20.i47.18022
- Cuesta MA. Review of different approaches of the left recurrent laryngeal nerve area for lymphadenectomy during minimally invasive esophagectomy. *J Thorac Dis.* (2019) 11:S766–70. doi: 10.21037/jtd.2018.12.52
- Li B, Li B, Jiang H, Yang Y, Zhang X, Su Y, et al. The value of enhanced CT scanning for predicting lymph node metastasis along the right recurrent laryngeal nerve in esophageal squamous cell carcinoma. *Ann Transl Med.* (2020) 8(24):1632. doi: 10.21037/atm-20-4991
- Lambin P, Rios-Velazquez E, Leijenaar R, Carvalho S, van Stiphout RG, Granton P, et al. Radiomics: extracting more information from medical images using advanced feature analysis. *Eur J Cancer.* (2012) 48(4):441–6. doi: 10.1016/j.ejca.2011.11.036
- Gillies RJ, Kinahan PE, Hricak H. Radiomics: images are more than pictures, they are data. *Radiology.* (2016) 278:563–77. doi: 10.1148/radiol.2015151169
- Le NQK. Hematoma expansion prediction: still navigating the intersection of deep learning and radiomics. *Eur Radiol.* (2024) 34:2905–7. doi: 10.1007/s00330-024-10586-x
- Le VH, Kha QH, Minh TNT, Nguyen VH, Le VL, Le NQK. Development and validation of CT-based radiomics signature for overall survival prediction in multi-organ cancer. *J digital Imaging.* (2023) 36:911–22. doi: 10.1007/s10278-023-00778-0
- Wang Y, Zhu L, Xia W, Wang F. Anatomy of lymphatic drainage of the esophagus and lymph node metastasis of thoracic esophageal cancer. *Cancer Manag Res.* (2018) 10:6295–303. doi: 10.2147/CMARS182436
- Tachimori Y. Pattern of lymph node metastases of squamous cell esophageal cancer based on the anatomical lymphatic drainage system: efficacy of lymph node dissection according to tumor location. *J Thorac Dis.* (2017) 9:S724–30. doi: 10.21037/jtd.2017.06.19
- Mizutani M, Murakami G, Nawata S, Hitrai I, Kimura W. Anatomy of right recurrent nerve node: why does early metastasis of esophageal cancer occur in it? *Surg Radiol Anat.* (2006) 28(4):333–8. doi: 10.1007/s00276-006-0115-y
- Ye K, Xu JH, Sun YF, Lin JA, Zheng ZG. Characteristics and clinical significance of lymph node metastases near the recurrent laryngeal nerve from thoracic esophageal carcinoma. *Genet Mol Res.* (2014) 13:6411–9. doi: 10.4238/2014.August.25.4
- Kato H, Kuwano H, Nakajima M, Miyazaki T, Yoshikawa M, Ojima H, et al. Comparison between positron emission tomography and computed tomography in the use of the assessment of esophageal carcinoma. *Cancer.* (2002) 94:921–8. doi: 10.1002/ncr.10330
- Billè A, Okiror L, Skanjeti A, Errico L, Arena V, Penna D, et al. Evaluation of integrated positron emission tomography and computed tomography accuracy in detecting lymph node metastasis in patients with adenocarcinoma vs squamous cell carcinoma. *Eur J Cardiothorac Surg.* (2013) 43(3):574–9. doi: 10.1093/ejcts/ezs366
- Ou J, Wu L, Li R, Wu CQ, Liu J, Chen TW, et al. CT radiomics features to predict lymph node metastasis in advanced esophageal squamous cell carcinoma and to discriminate between regional and non-regional lymph node metastasis: a case control study. *Quant Imaging Med Surg.* (2021) 11:628–40. doi: 10.21037/qims-20-241
- Li H, Chen TW, Li ZL, Zhang XM, Chen XL, Wang LY, et al. Tumour size of resectable oesophageal squamous cell carcinoma measured with multidetector computed tomography for predicting regional lymph node metastasis and N stage. *Eur Radiol.* (2012) 22(11):2487–93. doi: 10.1007/s00330-012-2512-4
- Li ZX, Liu XB, Li Y, Liang GH, Wang ZF, Zheng Y, et al. [Application value of CT examination of lymph node short diameter in evaluating cardia-left gastric lymph node metastasis in thoracic esophageal squamous cell carcinoma]. *Zhonghua Zhong Liu Za Zhi.* (2023) 45(11):962–66. doi: 10.3760/cma.j.cn112152-20220313-00173
- Ng F, Ganeshan B, Kozarski R, Miles KA, Goh V. Assessment of primary colorectal cancer heterogeneity by using whole-tumor texture analysis: contrast-enhanced CT texture as a biomarker of 5-year survival. *Radiology.* (2013) 266:177–84. doi: 10.1148/radiol.12120254
- Liu Y, Zou ZQ, Xiao J, Zhang M, Yuan L, Zhao XG. A nomogram prediction model for recurrent laryngeal nerve lymph node metastasis in thoracic oesophageal squamous cell carcinoma. *J Thorac Dis.* (2019) 11:2868–77. doi: 10.21037/jtd.2019.06.46
- Hong TH, Kim HK, Lee G, Shin S, Cho JH, Choi YS, et al. Role of recurrent laryngeal nerve lymph node dissection in surgery of early-stage esophageal squamous cell carcinoma. *Ann Surg Oncol.* (2022) 29(1):627–39. doi: 10.1245/s10434-021-10757-w
- Betancourt-Cuellar SL, Benveniste MFK, Palacio DP, Hofstetter WL. Esophageal cancer: tumor-node-metastasis staging. *Radiol Clin North Am.* (2021) 59(2):219–29. doi: 10.1016/j.rcl.2020.11.008
- Li H, Zhu Y, Burnside ES, Huang E, Drukker K, Hoadley KA, et al. Quantitative MRI radiomics in the prediction of molecular classifications of breast cancer subtypes in the TCGA/TCIA data set. *NPJ Breast Cancer.* (2016) 2:16012. doi: 10.1038/npjbcancer.2016.12